A Little Big Bang scenario of fragmentation

X. Campi, H. Krivin, E. Plagnol, N. Sator

A "Little Big Bang" Scenario of Multifragmentation

X. Campi, H. Krivine,
LPTMS[*], F-91405 Orsay Cedex, France
E. Plagnol[†]
Collège de France/PCC, F-75231 Paris Cedex 05, France
and
N. Sator[‡]
Dipartimento di Fisica, Università di Napoli "Federico II",
INFM Napoli, Via Cintia, 80126 Napoli, Italy

December 12, 2002

Abstract

We suggest a multifragmentation scenario in which fragments are produced at an early, high temperature and high density, stage of the reaction. In this scenario, self-bound clusters of particles in the hot and dense fluid are the precursors of the observed fragments. This solves a number of recurrent problems concerning the kinetic energies and the temperature of the fragments, encountered with the standard low density fragmentation picture. The possibility to recover the initial thermodynamic parameters (T and ρ) from the inspection of the asymptotic fragment size and kinetic energy distributions is discussed.

1 Introduction

Recent theoretical studies of the morphology of simple fluids have suggested the presence of self-bound clusters of particles [1, 2, 3]. The (time averaged) mass distributions of these clusters depend essentially on the energy and density of the system and resemble those found in nuclear multifragmentation (U-shapes, power law, exponentials). Furthermore, these distributions (event averaged) remain invariant if the system is allowed to expand freely.

[*]UMR 8626, CNRS Université de Paris XI
[†]eric.plagnol@cdf.in2p3.fr
[‡]Present adress : LPTL, Université de Paris VI, 4, place Jussieu 75252, Paris Cedex 05 France

The above observations suggest the following scenario for multifragmentation: In a first step, the nucleus is excited (and possibly compressed). In this "hot" and dense phase, at least part of it reaches thermal equilibrium. Clusters, defined as self-bound ensembles of particles, are present in this medium. Immediately after, the system starts to expand, out of equilibrium, as *an ensemble of interacting clusters*. Asymptotically, these *clusters* cease to interact with each other, becoming the observed *fragments*. The sudden expansion reveals the cluster distribution of the primordial hot and dense phase of the system (*a Little Big Bang*) and "freezes" it. The long range Coulomb repulsion between clusters helps this freezing process. The smallness of the system also helps, because most of the clusters are close to the surface and escape freely into the vacuum. The clusters have ramified shapes in the dense medium and become, at asymptotic times, spherical fragments.

The "standard" mechanism [4, 5, 6, 7] of multifragmentation, adopted in the so-called "Statistical Equilibrium Models" (SEM), is different: Once the system is excited, it undergoes an homogeneous and quasi-static expansion. At some sufficiently low density (freeze-out), it "recondensates" as *an ensemble of spherical non-overlapping and non-interacting fragments*. At this stage, the models calculate the fragment mass distributions as those of a gas of non-interacting fragments with internal nuclear structure, at equilibrium. These models have been extremely successful in describing the observed fragment mass distributions [7, 8]. It is however important to notice that the main hypothesis (equilibrium at low freeze-out density, spherical fragments) required in these models to make the calculations feasible, are not substantiated by other, more microscopic, approaches of the multifragmentation phenomenon [9, 10, 11, 12, 13]. In fact, despite the success in describing the mass distributions, this "standard" scenario leads to some recurrent problems. Among them, the most important is the prediction of the kinetic energies of the fragments that are too low compared with experimental observations [14, 15]. This problem is "corrected" by adding an *ad hoc* radial flow to the fragments. However the origin of this flow is unclear and seems inconsistent with the hypothesis of equilibrium and the low freeze-out density. Another problem concerns the internal temperature of the fragments, which in the experiments seems to be much lower than the temperature of the gas of fragments [16, 17]. We will see that the proposed high density scenario with pre-existing clusters helps to solve these problems in a very natural way.

This approach is substantiated by Classical Molecular Dynamics (CMD) calculations [1, 2, 9, 10, 11] of an ensemble of particles either confined in a container or freely expanding. Our goal is to interpret the (well known) results obtained with these methods at the light of our present knowledge on clusters in hot and dense fluids. We are thus not proposing a well-finished model of nuclear multifragmentation which could be directly compared with experimental data, but rather a generic scenario.

This paper is organized as follows. In section 2, we present results on the mapping between thermodynamics and clustering in dense and confined medium, in large and in nuclear-size systems. In section 3 we discuss the free expansion of these latter systems. Some final remarks will be found in Section

4.

2 Clusters in Confined Systems

In order to investigate the mapping between thermodynamics and clustering, we first have to define what a physical cluster is, over the whole range of densities and temperatures. A definition solely based on a proximity criterium (interaction radius) in configuration space is obviously not adequate at high densities and/or temperatures.

At low density, a cluster is naturally defined as a self bound ensemble of particles. By continuity we shall extend this definition to a dense medium. Several approaches can be used to identify self-bound clusters among the particles of the system. For instance, they can be defined as a partition of particles which minimizes the interaction energy between clusters [18, 19]. Clusters can also be built, bond by bond, using Hill's criterium [20]: Two particles are bound if their relative kinetic energy is less than their potential energy. In other words, a cluster is a set of particles close to each other in phase space and *not only* in configuration space. It must be emphasized that, with this model, knowing the positions and velocities of the particles, no adjusting parameter is necessary to recognize the clusters whatever the density or the temperature. In previous works [1, 2, 3], we checked that the cluster size distribution does not depend significantly on the specific definition of self-bound clusters mentioned above.

The mapping between thermodynamics and clustering can be studied by performing classical microcanonical molecular dynamic simulations of a simple fluid. Particles confined in a cubic container interact through a Lennard-Jones potential ($V(r) = 4\epsilon((\sigma/r)^{12} - (\sigma/r)^6)$), where ϵ and σ define the energy and length scales respectively. The natural time-unit is defined by $\tau_0 = \sqrt{m\sigma^2/(48\epsilon)}$, where m is the mass of the particles. When Coulomb interaction is included, it is done with the prescription of reference [9]. Self-bound clusters are recognized by means of Hill's criterium. The details of the calculations can be found in references [1, 2, 3].

In order to establish an accurate mapping between thermal and geometrical properties of this fluid, we first present results for the case of a large system ($N \simeq 12000$ particles) with periodic boundary conditions [1] (and, of course without Coulomb interaction):

- When crossing the condensation curve at sub-critical densities, a macroscopic cluster appears in the liquid-gas coexistence region[1]. Although defined in a complete different theoretical framework, our clusters mark the liquid-gas coexistence line as Fisher's clusters do [21][2].

- A percolation line starts at the thermodynamical critical point (within the uncertainties inherent to the critical slowing down) and goes through

[1] This correspondence between thermodynamics and clustering is not observed when clusters are simply defined by a constant interaction radius in the configurational space.

[2] Notice however that Fisher's clusters are non-interacting and not microscopically defined.

the supercritical region of the phase diagram. Thus, a power law behavior of the cluster size distribution does not necessarily imply that the system is in its thermodynamical critical state. Also notice that this percolation line does not extend below the critical temperature.

- It can be shown that the Hill prescription we are using to define self-bound clusters in a realistic fluid is equivalent [22] to the prescription introduced by Coniglio and Klein [23] to define physical clusters in the lattice-gas model. This gives a theoretical framework to understand the existence of this critical line. Along this line (usually called Kertész line), the critical exponents are those of the random percolation, except at the thermodynamical critical point, where the exponents are those of the correlated percolation [23].

- The energy of the system is nearly constant along the critical percolation line.

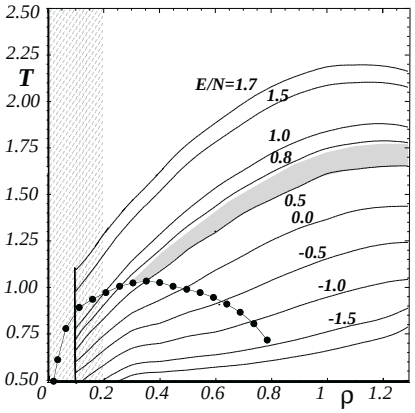

Figure 1: *Phase diagram of a Lennard-Jones fluid (including Coulomb interaction) of* $N = 189$ *particles confined in a container. The position of the coexistence line is sketched by filled dots. Lines of equal energy are indexed by the energy per particle of the system. The shaded area indicates the location of the percolation critical region. The dashed area shows tentatively the domain of application of the standard SEM. Temperature* T *and density* ρ *are in units of the Lennard-Jones parameters (*ϵ *and* σ*). The full circle indicates the critical point.*

These results remain valid in small systems [2]. We have studied the behaviour of small systems like atomic nuclei by performing similar calculations with $N = 189$ particles confined in a cubic container with perfectly reflecting walls and interacting *via* a Lennard-Jones potential plus Coulomb. The "phase diagram" is represented in figure 1. Although the sharp effects found in the thermodynamical limit are smoothed by the finite size and surface effects, we reach basically the same conclusions.

- As is shown in figure 2, the shape of the cluster size distribution changes

suddenly when crossing the condensation curve for a very small variation of temperature.

- The cluster size distribution presents a power law behavior along a percolation "line" (more precisely a band due to the finite size effects) which starts at the thermodynamical critical point (region) (see figure 1). Along this line, the slope of the cluster size distribution ($\tau \simeq 2.5$) is in accordance with percolation theory[3].

We note also that, in the supercritical region, a given cluster size distribution corresponds qualitatively to a given energy of the system. We stress that the converse is not true, notably below the coexistence line.

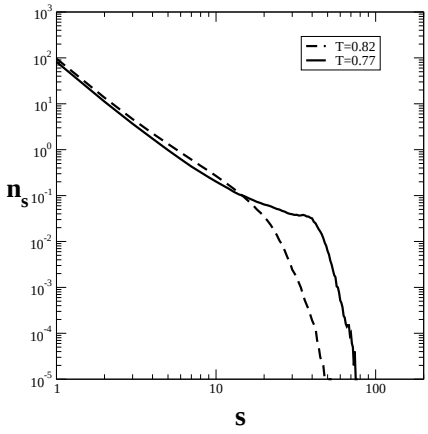

Figure 2: *Cluster size distributions n_s just above ($T = 0.82$) and below ($T = 0.77$) the coexistence "line" at $\rho = 0.1$ for a system of $N = 189$ particles.*

Studying the degrees of freedom associated to the internal motion of the particles inside the clusters, and the degrees of freedom associated to the center of mass motion of these clusters, we define two "effective temperatures", $T^*(s)$ and $T^{cm}(s)$, as two third of the average kinetic energy of the corresponding ensemble [4]. Let us define the internal velocity v^* as the velocity of a particle calculated in the center of mass system of the cluster it belongs to. As is shown in Fig 3, the internal velocity distribution for cluster of size $s = 2$ contrasts strongly with a Maxwell distribution. As it should be, by definition of the self-bound clusters, the distribution is truncated at $v^* = 1$. However, increasing the cluster size, the velocity distribution tends to a Maxwell distribution characterized by the asymptotic temperature $T^*(s)$ for $s > 50$ (see figure 4). Similar results [24]

[3]Due to the range of our potential, in a small system, all particles interact with each other, so the mean field result is expected.

[4]However, if we were able to isolate a cluster from the others (this is what happens during the expansion), the internal effective temperature would become the real thermodynamic temperature of the isolated fragment.

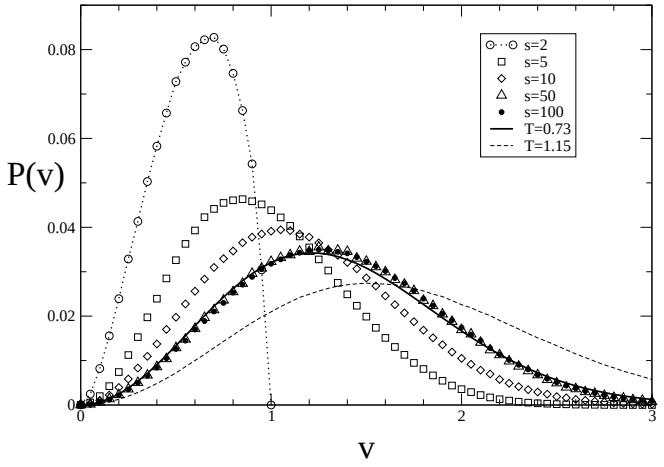

Figure 3: *Internal velocity distribution for different cluster sizes s (for* $\rho = 0.50$ *and* $T = 1.15$*). For the purposes of comparison, the Maxwell distribution function is represented for* $T = 1.15$ *(temperature of the system) and for* $T = 0.73$ *(asymptotic internal effective temperature of the clusters, see figure 4).*

have been recently obtained by calculating the first order corrections (namely the interaction between a monomer and a self-bound cluster) to a perfect gas of clusters at low density. Whatever the size of the clusters and the thermodynamic state of the system, the internal effective temperature $T^*(s)$ is always less than the (real) temperature of the fluid. On the other hand, the effective temperature associated to the "gas of clusters", T^{cm} is greater than the (real) temperature of the fluid. In figure 4, we illustrate this inequality which was already mentioned [24]. In brief, the system can be seen as a *"hot" gas of "cold" physical clusters.*

The present results show that various basic hypothesis of the SEM [5, 7] are not fulfilled. These models consider an ensemble of spherical, non-interacting clusters, with an internal temperature equal to the one of the global system, confined in a volume at low densities ($\rho \sim 0.2$). On the contrary, we find that:

1. The clusters exhibit fractal shapes in the confined system[5] (see figure 5, left). We must point out that it is not incompatible with the cold spherical fragments we expect at the end of the expansion. Indeed, by following the evolution of a self-bound cluster during the expansion (cf section 3) we find that it becomes spherical as it should be (see figure 5, right).

2. Even at densities as low as $\rho = 0.1 - 0.2$, the strong interaction (without Coulomb) between clusters still represents about 40 % of the total

[5] As it should be, in large systems ($N = 12000$), the fractal dimension ($D_f = 2.55$) of the self-bound clusters along the percolation line has been checked to be in agreement with the one of random percolation [3].

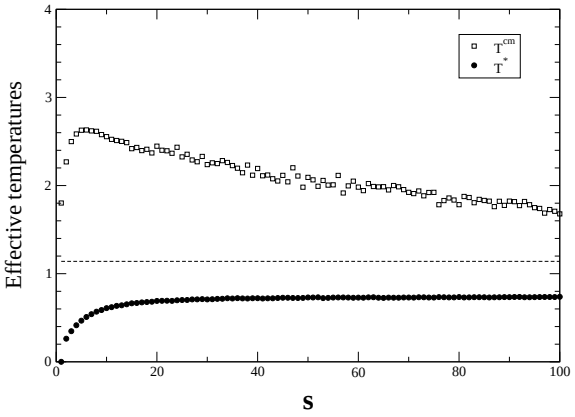

Figure 4: *Effective internal temperature of clusters $T^*(s)$ and temperature of the gas of clusters $T_{cm}(s)$ as a function of the cluster size s, for $\rho = 0.50$ and $T = 1.15$. The real temperature of the fluid (dashed line) is indicated for comparison. The system contains $N = 189$ particles.*

potential energy.

3. The internal temperature of the clusters is lower than the temperature of the system. Thus, this fragments will become in the course of the expansion (see next section) the observed fragments, without significant particle evaporation.

Usually three observables are used to extract the temperature from nuclear experimental data: i) the kinetic energies of the fragments, ii) the population of the excited states of fragments [16] and iii) the ratio of isotopic yields [27]. All these methods assume that these observables will yield the thermodynamic temperature of the system, T. Our study contradicts this. As shown in figure 5, the internal and "kinetic energy" temperatures of the fragments are not a measure of T.

3 Fragments in Expanding Systems

Having studied the properties of clusters in confined systems, we now turn to the problem of their evolution once the system is allowed to expand freely. The questions we want to address are :

- How and when do the fragments appear ? Does the asymptotic fragment size distribution and kinetic energies relate to the initial configuration or to an intermediate freeze-out configuration ?

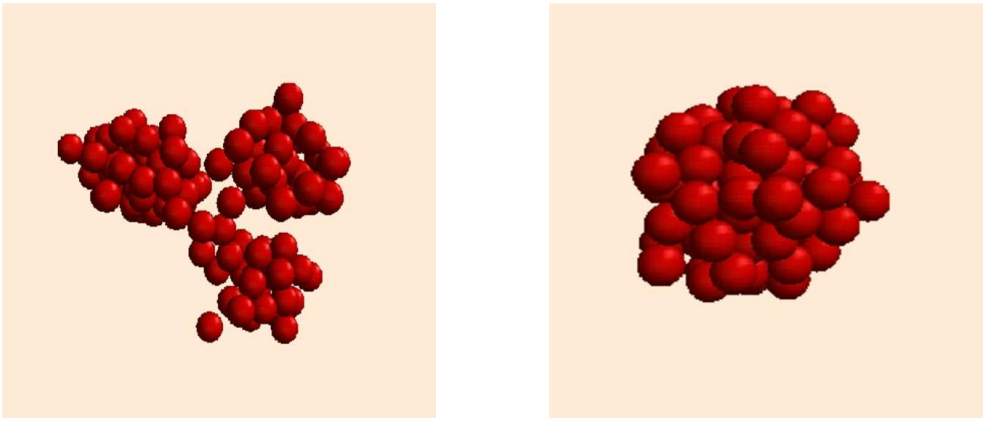

$t = 0$ $t = 400\tau_0$

Figure 5: *Typical shape of the largest cluster in the confined medium ($t = 0$) and at asymptotic times after expansion ($t = 400\tau_0$).*

- Does the system follow a quasi-static path up to some, low density, freeze-out configuration where the final fragment distribution would be determined, as assumed in the standard [4, 5, 6, 7] models ?
- How can the temperature and density of this initial configuration be inferred from the information measured at asymptotic times ?

In order to answer these questions, we have analyzed a number of expansions of the system using the CMD with Lennard-Jones plus Coulomb potentials [9]. The system is characterized, as in section 2, by its energy (microcanonical ensemble), its density and the number of particles. It is enclosed in a cubic container with perfectly reflective walls. The calculations proceed in two steps :

- After a thermalisation period, the container is removed at a time defined as $t = 0$.
- The system is then allowed to expand freely during a period of time sufficient to establish the final (asymptotic) fragment size distribution.

Let us first examine the time evolution of the components of the energy. Figure 6 displays, the evolution of the L-J potential energy, the Coulomb energy, the total kinetic energy and the total energy. At $t = 0$, the effect of the opening of the container is clearly visible by a rapid decrease of the potential energy. This corresponds to the fact that the mean distance between clusters increases rapidly. It can be noted that the asymptotic potential energy does not go to zero, indicating the existence of fragments of finite size. The kinetic energy shows a complementary behaviour : after a sharp decrease, the Coulomb acceleration is clearly observed.

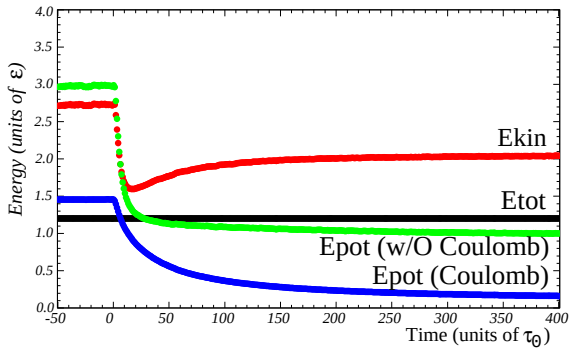

Figure 6: *Energies as a function of time for a CMD calculation performed for* $E_{tot} = 1.2$, $N = 189$ *and* $\rho = 0.8$. *Are shown the total energy, the total kinetic energy, the potential energy (absolute value, not including Coulomb) and the Coulomb potential energy. The container is removed at time t=0 (see text).*

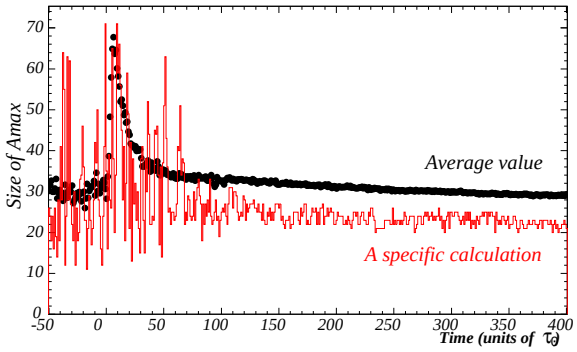

Figure 7: *Time evolution of the size of the largest fragment. Full dots correspond to the average values for a 100 calculations, the line to a specific calculation. The container is removed at time* $t = 0$ *(see text). CMD calculations with* $E_{tot} = 1.2$, $N = 189$ *and* $\rho = 0.8$.

We shall now study the evolution of the size of the largest fragment (Figure 7). The line gives the result of a single event whereas the full dots represent an average over 100 expansions. The striking feature of this figure is the observation that the average value of the largest *fragment* at asymptotic times is very close to the average value of the largest *cluster* identified in the container ($t < 0$). The correspondence between the largest cluster in the container (time average) and the asymptotic largest fragment (event average) is systematically observed. This conclusion is valid for all the calculations that we have performed, independently of the initial density and energy.

Figure 8 shows confirmation of this conclusion by the examination of more detailed quantities. It presents the fragment size distributions as a function of time. To within statistical fluctuations, one observes that they are almost

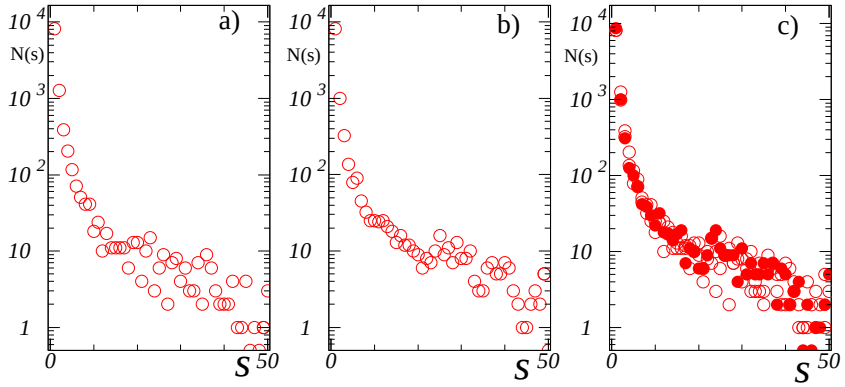

Figure 8: *Fragment size distribution averaged over* 100 *events for* $t = 0$, $200\tau_0$ *and* $400\tau_0$. *CMD calculations with* $E_{tot} = 1.2$, $N = 189$ *and* $\rho = 0.8$. *The figure a) corresponds to* $t = 0$, *b) to* $t = 200\tau_0$ *and c) to* $t = 400\tau_0$. *Full circles indicate the superimposed results of a) and b).*

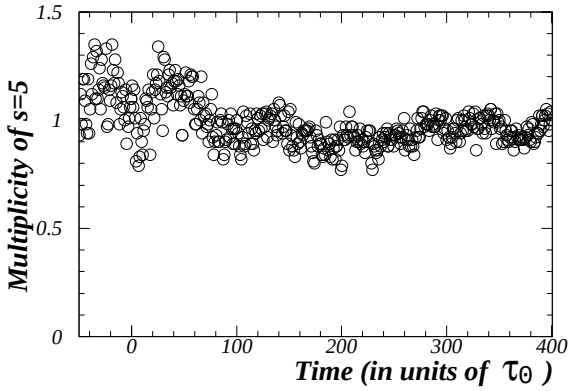

Figure 9: *Average multiplicity of fragments of size* $s = 5$ *as a function of time. The container is removed at time* $t = 0$ *(see text). CMD calculations with* $E_{tot} = 1.2$, $N = 189$ *and* $\rho = 0.8$.

identical. Figure 9 shows the evolution in time of the multiplicity of fragments of size $s = 5$. There again, the asymptotic value is very close to the initial one. In view of the rapid decrease of the fragment size distribution observed (figure 8), the stability of this quantity is impressive.

The correlation between the initial and final size distributions is, we believe, a consequence of the violent expansion phase (which follows the opening of the container), the small size of the system and the presence of the Coulomb repulsion between the clusters. Because of the small size of the system, the fragments are always close to the surface and will escape freely into the vacuum. For a

very large system, the expansion phase would give rise, in the central region, to substantial thermal and chemical activity and hence modify the thermodynamic parameters of the system. In a small system, this modification appears almost unobservable. The influence of the expansion phase is enhanced by the presence of the Coulomb force. The Coulomb potential not only accelerates the expansion but also introduces, between the fragments, a Coulomb barrier, which inhibits particle exchanges.

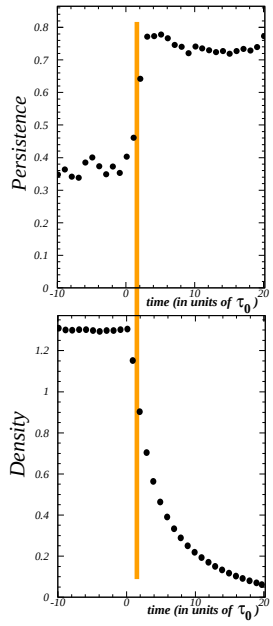

Figure 10: *Persistence (see text) of fragments of size $s > 3$ and density of the expanding system, as a function of time. $E_{tot} = 1.2$, $N = 189$ and $\rho = 1.3$.*

The violence of the expansion phase is illustrated by the figure 10 which shows the *persistence* of fragments and the density of the system, as a function of time. The persistence is defined as the fraction of the number of particles present in a given fragment which will remain in this fragment at asymptotic times ($t = 400\tau_0$). The density, a poorly defined quantity in such an inhomogeneous expansions, is deduced from the r.m.s. radius of an uniformly charged sphere of the same Coulomb energy. Figure 10 shows that this persistence evolves very rapidly and almost reaches its asymptotic value at densities of the order of 0.8: An exchange of particles between fragments is clearly observed during this (short) period, but this limited chemical activity does not induce a modification of the average size of the fragments.

The picture that comes out from these calculations therefore corresponds to a fast, non equilibrium, expansion of a gas of clusters. This expansion acts as a "developer" of the presence of these clusters, the Coulomb repulsion helping

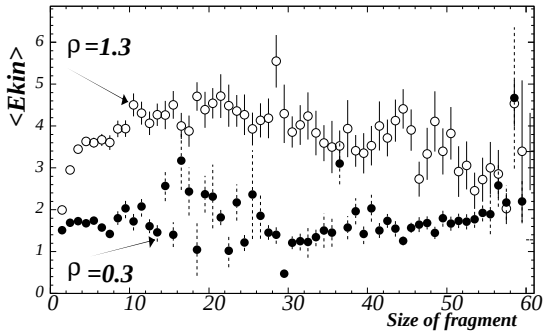

Figure 11: *Distributions of the kinetic energies as a function of the fragment size for a CMD calculation with $E_{tot} = 0.2$, $N = 189$ and densities of 1.3 (empty dots) and 0.3 (full dots). Calculations does not include Coulomb interaction.*

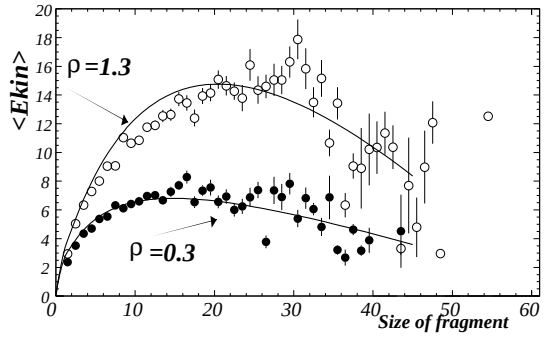

Figure 12: *Same as figure 11, but with Coulomb interaction. Remark the difference in the E_{kin} scales. See text for the meaning of the solid line.*

to "fix" them. Thus, the (event) average distribution of fragments reflects the (time) average distribution of clusters in the dense and hot initial state.

We now study the kinetic energies of the fragments. Figure 11 shows the asymptotic kinetic energy of expansions *without* Coulomb interaction ($E_{tot} = 0.2$). As can be seen, the kinetic energies obtained from different starting densities (0.3 and 1.3) are quantitatively different. This demonstrates once more that the expansion is a non-equilibrium phenomenon. If equilibrium, at a given energy, was maintained during the expansion, the system starting from $\rho = 1.3$ would, at a point in time, reach the same point in $\{T - \rho\}$ space as the one from which the system at $\rho = 0.3$ starts and hence the two systems would be indistinguishable in all respect: Figure 11 demonstrates that it is not the case.

Figure 12 shows the kinetic energies in the case *with* Coulomb interaction. The shape of these distributions is characteristic of the presence of Coulomb forces and is close to what is observed in nuclear reactions at Fermi bombarding energies ($\sim$ 50 MeV/A) for symmetric nuclei [14, 25]. The solid lines show a

qualitative (analytical) prediction of what would be expected in the case of a uniformly charged medium.

The important feature that is revealed by this figure is the dependence of the kinetic energies on the initial density. This result appears to confirm the evolution suggested by the analysis of the fragment size distribution. Very rapidly after the removal of the container, the fragments cease to strongly interact with the medium and are accelerated by the (Coulomb) repulsive potential. Because this expansion takes place out of equilibrium, the Coulomb energy does not transform into thermal energy but in fragment kinetic energy. The higher the density of the initial configuration, the greater the final kinetic energies are. We can therefore consider that the asymptotic kinetic energies are a "measure" of the density at which the systems departs from equilibrium.

This scenario accounts, at least partially, for the radial flow often associated with multifragmentation processes [14, 25]. As stated above (section 1), the standard method of analysis, using the SEM, assumes a low density configuration and therefore naturally underpredicts the kinetic energies of the fragments when the system has evolved (out of equilibrium) from a high density state. To compensate for this, an extra component of "radial flow" is artificially introduced. In the scenario we suggest, such an extra flow is not necessary when the calculation is performed at the correct initial density. It is important to remark that our scenario does not necessarily imply large values for the kinetic energy. For example, for peripheral heavy ion reactions, no initial compression is expected. Even more, for proton-nucleus or π-nucleus collisions, initial densities lower than the normal equilibrium nuclear density are plausible because of the formation of holes inside a nucleus with normal volume [26].

Having "measured" the density, we now turn to the estimation of the temperature. The sensitivity of the kinetic energies to the density, provides a "method" to determine the thermodynamic parameters of the point at which the system departs from equilibrium. The analysis of the fragment size distribution will select which iso-$n(s)$ line is to be considered. The analysis of the kinetic energies will determine the density. The intersection of both will yield T and ρ. Evidently, this method is physics (model) dependent, i.e. it is only if one is able to calculate the relationship $E(T, \rho)$ and the fragment size distribution at each (T, ρ) point that the thermodynamical parameters can be extracted from the analysis of the data measured at asymptotic times.

4 Final remarks

We have explored a new scenario of multifragmentation, based on the observation that a dense and hot fluid, at equilibrium, can be viewed as a hot gas of cold clusters. These clusters are defined as self-bound ensembles of particles. When the system is allowed to expand freely, it proceeds, *out of equilibrium*, as an ensemble of interacting clusters. Once these clusters cease to interact with each other, they become the observable fragments.

We believe that this "Little Big Bang" scenario is not only more realistic

than the "standard" low density freeze-out model but that it also allows to solve a number of recurrent problems:

- Equilibrium is assumed only at the beginning of the process, when the high density and temperature make this assumption more likely. No "quasi-static" hypothesis of expansion up to a low freeze-out density is needed.
- Due to this compacity, the Coulomb repulsion between fragments generates larger kinetic energies. Clusters in the dense medium have "ramified" (fractal in large systems) forms, allowing more compact configurations in the initial stage. The observed radial flows can thus be explained, at least partially, in a natural way.
- Isolated fragments are cold, because the precursor clusters are already cooler than the ensemble of the system.

The aim of this work was to present a new scenario of multifragmentation, not a well finished model producing results directly comparable with experimental data. One has to keep in mind that the present scenario is supported by classical molecular dynamics simulations of the expansion of a system of particles interacting through Lennard-Jones plus Coulomb potentials, initially confined in a container. Although we believe that these results are generic for describing the free expansion of any simple fluid (and that nuclear matter at high temperatures behaves as a simple fluid), it is necessary to confront our results with other calculations. Namely, with Quantum Molecular Dynamics [12, 13] calculations to test the equilibrium hypothesis in the first stages of the reaction, and with Fermionic Molecular Dynamics [28] to check the importance of quantum effects, particularly at sub-critical temperatures.

We would like to thank F. Lavaud for his contribution to the expansion phase calculations. One of us (N.S.) wishes to acknowledge financial support of the European TMR Network-Fractals (Contract number: FMRXCT-980183).

References

[1] X. Campi, H. Krivine and N. Sator, Physica A **296**, 24 (2001).

[2] X. Campi, H. Krivine and N. Sator, Nucl. Phys. A **681**, 458c (2001).

[3] N. Sator, "Clusters in simple fluids", Phys. Rep., to be published.

[4] D.H.E. Gross, Phys. Rep. **279**, 119 (1997).

[5] J.P. Bondorf, A.S. Botvina, A.S. Iljinov, I.N. Mishustin, and K. Snepen, Phys. Rep. **257**, 133 (1995).

[6] W. A. Friedman, Phys. Rev. C**42**, 667 (1990).

[7] A. S. Botvina et al., Nucl. Phys. A**584**, 737,(1995).

[8] R. Bougault et al., Proc. Int. XXXV Winter Meeting on Nuclear Physics, Bormio (Italy) (1997) ; S. Salou, Ph.D thesis University of Caen (France) (1997) GANIL T 97 06.

[9] T.J. Schlagel and V. R. Pandharipande, Phys. Rev C**36**, 162 (1987).

[10] V. Latora, M. Belkacem, A. Bonasera, Phys. Rev. Lett. **73**, 1765(1994).

[11] A. Chernomoretz, M. Ison, S.Ortiz and C. O. Dorso, Phys. Rev. C**64**, 024606 (2001).

[12] J. Aichelin, Phys. Rep. **202**, 233 (1991).

[13] R. Nebauer and J. Aichelin, Nucl. Phys. A**681**, 353c (2001).

[14] N. Marie et al., Phys. Lett. B**391**, 15 (1997).

[15] G.J. Kunde et al., Phys. Rev. Lett. **74**, 38 (1995).

[16] M. B. Tsang, W. G. Lynch and W. A. Friedman, Phys. Rev. Lett. **78**, 3836 (1997).

[17] V. Serfling et al., Phys. Rev. Lett. **80**, 3928 (1998).

[18] C. Dorso and J. Randrup, Phys. Lett. B **301**, 328 (1993).

[19] A. Puente, Phys. Lett. A **260**, 234 (1999).

[20] T.L. Hill J. Chem. Phys **23** 617 (1955).

[21] M.E. Fisher, Physics **3**, 255 (1967).

[22] X. Campi and H. Krivine, Nucl. Phys. A **620**, 46 (1997).

[23] A. Coniglio and W. Klein, J. Phys. A: Math. Gen. **13**, 2775 (1980).

[24] R. Soto and P. Cordero, Physica A, 521 (1998).

[25] F. Lavaud, PhD Thesis, University of Orsay, IPNO-T.01-06, (2001).

[26] J.J. Gaimard and K. H. Schmidt, Nucl. Phys. A **531**, 709 (1991).

[27] S. Albergo et al. Nuovo Cimento A**89**, 1 (1985).

[28] H. Feldmeier, Nucl. Phys. A**681**, 398c (2001).